Response to Referees

Evaluation of semi-implicit and explicit sedimentation approaches in the two-moment cloud microphysics scheme of ICON

Simon Bolt, Nadja Omanovic

December 1, 2025

Dear editor and referees,

We would like to thank the editor for handling our manuscript and the referees for their careful evaluation of the revised manuscript. Below we address our detailed responses to all the comments. In this response-to-review document we try to clarify and address each of the suggestions, comments, and questions made during the review process. Therefore we have copied the comments in lavender boxes and have addressed them one by one. In the response we use italic fonts to quote text from the revised manuscript. Additional to the revised manuscript, we have uploaded a version of the manuscript with highlighted tracked changes.

Best regards, Simon Bolt, and Nadja Omanovic

Response to Ted Mansell (CC1)

Just a quick comment for the authors. I highly recommend adding a profile of the reflectivity moment to Figure 3. The mean diameter alone does not tell us about excessive size sorting, but Z definitely does. Relying on low-order diffusion is really not a great solution, and as you show, vertical grid spacing and the Courant number play a strong role. It can smooth out the shock, but that is only part of the problem because the leading edge is still there. Whatever is done, however, showing Z is important so that the reader can at least see whether it increases (i.e., sorts excessively) or not. Having excessive sorting in the result doesn't necessarily distort rain rates etc., but it can be detrimental for assimilation of radar reflectivity by causing biases.

The common strategy of placing limits on the slope parameter or mean size only treats excessive sorting at the point where reflectivity is becoming unrealistic, but doesn't fix the underlying problem. Of course, I would advocate using a temporary Z moment in the sedimentation to adaptively adjust N while conserving mass. But all that is really needed here is to show what the given schemes are doing, and showing Z would give a more complete picture of that.

yours,
Ted Mansell

Thank you for the suggestion! We modified Fig. 3 to include the diagnostic reflectivity (dBZ), and added the following sentence to the text (line 326):

" *Considering the reflectivities in Fig. 3, the solutions with very low resolution result in a maximum reflectivity close to the spectral solution but a too large vertical spread, whereas higher resolutions produce too high reflectivity maxima at the leading edge.* "

Response to anonymous referee #1

Comments to the Authors

The paper compares the two numerical schemes to solve sedimentation that are implemented in the two-moment scheme of ICON: a semi-imcplicit one and an explicit one. The overall quality of the paper is good: the topic is interesting, the experiments are well designed and the conclusions are well sustained. I only have some doubts about the reference solution presented in the second experiment (see below). Another important

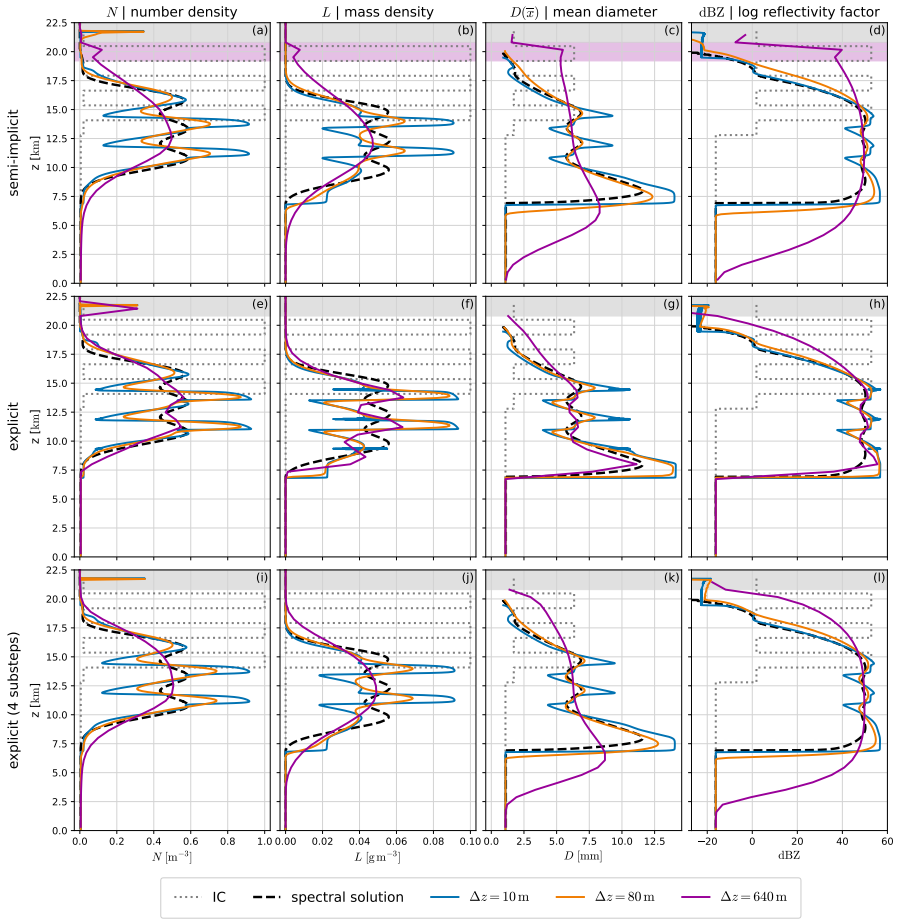

Figure 3: Hydrometeor profiles (N, L, diagnostic mean diameter, reflectivity) in a pure sedimentation case after $t_{\text{end}} \approx 534\,\text{s}$, for three different mesh resolutions and numerical schemes, in addition to the reference spectral solution. The diameter is only drawn where $L > q_{\text{crit}} = 10^{-9}\,\text{kg}\,\text{m}^{-3}$. In the area shaded gray, spikes induced by the operator $\mathcal{D}$, defined in Eq. (27), are visible. The region shaded purple highlights numerical artifacts caused by the flux limiter defined in Eq. (13). Setup details are provided in Sect 3.2.

issue is the lack of information in several parts of the text. Some important information is only provided in the figure captions, which makes it difficult to read the paper.

We thank the referee for the positive and constructive comments and we will address the detailed comments below. To improve readability in Section 3 (idealized experiments), we have moved the experiments' description from the figure captions to the text, in addition to several changes in response to the detailed comments of both referees. We now also include more information in several parts of the paper, e.g., we introduced a Table listing the relevant hydrometeor parameter choices (Table 2), and addressed the referee's concerns regarding the spectral reference solution. This is discussed in the detailed comments below.

Detailed comments

1) The authors should explain why the spectral solution in the second experiment (Figures 2 and 3) is considered the reference. While spectral methods are clearly better at representing changes in the size distribution, the sedimentation scheme typically suffers from diffusion like the standard two-moment scheme. This is seen in the leading edge of the spectral solution in Figure 3, where the diameter smoothly goes to zero. The authors should explain how the spectral solution is calculated (which resolution, which numerical scheme, which dt). One idea to show that diffusion is negligible for the spectral scheme would be to show how the spectral scheme deals with the linear advection case of the first experiment.

Thank you for this comment; we fully agree that this was not clear enough. We have now added explanations for

how we computed the spectral solution (line 298):

" *When considering sedimentation in the two-moment scheme, the numerical solutions of Eq. (9) should best be compared against a direct solution of the original spectral budget equation, Eq. (1). We compute such a reference by combining a bin method with analytical solutions of the linear advection equation: First, the initial conditions are decomposed into spectral components, i.e.,* 10 000 *equally spaced mass bins, such that (at least)* 99.9 % *of all particles are inside the region that is covered by the bins. Following that, each bin's respective number density is advected using an analytical solution of the linear advection equation with velocities given by Eq. (6). The number distribution obtained from those advected bins is then used to determine the first two moments and reflectivity for comparison with the numerical two-moment scheme solutions.* "

In that sense, applying our spectral scheme to the linear advection case simply means advecting a single bin with the superimposed velocity. Since we use the analytical solution for the advection part (and not a numerical method), we just recover the exact solution, which obviously does not suffer from numerical diffusion.

The fact that the diameter smoothly goes to (almost) zero in the spectral solution shown in Fig. 3 is therefore not caused by undesired diffusive properties; instead, it simply arises from our initial conditions: The initial conditions are never actually zero; their lowest values were chosen as 0.5% of the square waves' peaks. This has exactly the effect that the diameter looks smoother where the almost-zero background starts to dominate over the very few, but very large hydrometeors coming from the square waves. We made this choice of IC for two reasons: First, we can avoid an explosion of the diameter to infinity (it would eventually stop after reaching the bin with the highest mass). We wanted to avoid showing such a diameter explosion, since it is just a consequence of the Γ-distribution's infinitely long tail; and the diameter reaches such high values only where practically no mass nor particles are present anyways. Second, the background hydrometeors help to avoid some artifacts in the numerical solutions that are caused by clipping the velocities to zero where $L \leq q_{\text{crit}}$ as shown in Eq. (26). We think trying to avoid those artifacts here can be justified, since we have argued that the tracer advection would almost immediately destroy the conditions necessary for such artifacts to develop in non-idealized scenarios.

In order to make it clearer that we have a small background as opposed to zero hydrometeors in the ICs, we have modified the text to include " *The initial conditions, consisting of three square peaks and a small nonzero background hydrometeor concentration, ...*" (line 312).

For completeness, we demonstrate here in Fig. R3 how Fig. 3 would look like when deleting the small concentration of background hydrometeors in the initial conditions.

2) Please describe the linear advection experiment in the text and not only in the caption. It would help if it were written that no two-moment scheme is used and it is just the sedimentation of a tracer with a prescribed velocity.

Thank you, we agree. We have split the idealized experiments into two subsections (3.1 and 3.2), including moving most of the caption to the text and describing the experiments in more detail. We have also made further modifications to the linear advection experiment, as you suggested three comments down. We list all the related changed there.

3) I suggest the authors to write the parameterization for the hail velocity and for the mass-diameter relationship in the appendix and not to cite an ICON file. This can help for a better understanding and better reproducibility. It is not that long.

We have introduced a new table that lists all hail and graupel parameters that are relevant for sedimentation (Table 2), and also described the mass–diameter relationship in the caption.

4) In the abstract and conclusion, the authors state: *finer grid resolutions may result in insufficient diffusion, especially for the explicit scheme.* I disagree with this sentence in the NWP context. Finer grid resolutions in the horizontal are usually not matched by similar refinements in the vertical, while dt decreases with dx/dy. For example, ICON runs operationally with the same vertical grid for 2km and 500m resolutions. A more relevant comparison would be by changing dt, while keeping dz constant. In the explicit scheme this is similar to sub-stepping, and I would guess that more diffusion is expected.

Thank you for catching that. In the explicit scheme, more diffusion is indeed expected when reducing the time step (due to horizontal grid refinement) without changing the vertical discretization. We also refer to the next comment for more details on the semi-implicit scheme's behavior in such cases. In the abstract, we now write (line 12):

" *Purely horizontal grid refinement leads to increased diffusion in the explicit scheme, whereas finer vertical*

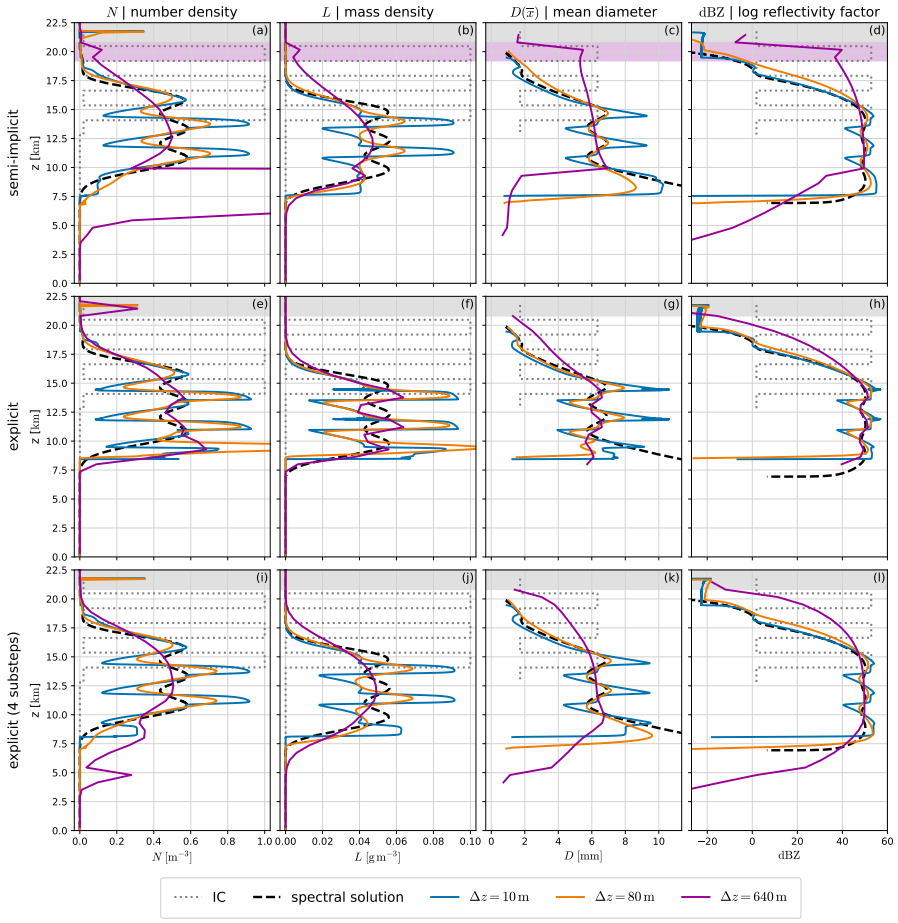

Figure R3: This is how Fig. 3 would look like when deleting the small concentration of background hydrometeors in the initial conditions.

resolutions may result in insufficient diffusion, especially for the explicit scheme. “

In the conclusions, we changed our statements similarly (line 499):

“ *If only the horizontal resolution is increased, the ensuing time step reduction will lead to more numerical diffusion in the explicit scheme, but leave the semi-implicit scheme largely unaffected. This is noteworthy, as it increases the similarity between the two sedimentation methods, thus rendering the explicit scheme more viable. Conversely, also increasing the vertical resolution results in reduced numerical diffusion for both schemes, which may become problematic for the explicit scheme due to the loss of smoothing capacity for oscillations that are either induced numerically or by the bulk parameterization.* “

5) Related to the previous point. Do you know what happens to the semi-implicit scheme when dt is reduced? (for the same dz). This could help to understand what happens at the higher resolution models.

Thank you for the suggestion; and indeed the two schemes behave differently in this regard. To show this, we have modified the linear advection experiment (Fig. 2) slightly by adding a semi-implicit configuration with smaller time step to show how the time step impacts this method when keeping Δz constant: Now, we simply show both the semi-implicit and explicit scheme with time steps $\Delta t = 10\,\mathrm{s}$ and $\Delta t = 2.5\,\mathrm{s}$. For consistency, we replaced the configuration “explicit (4 substeps)“ that was using $\Delta t = 10\,\mathrm{s}$ with “explicit ($\Delta t = 2.5\,\mathrm{s}$)“; those are practically equivalent in this linear advection case as mentioned in the figure’s caption. The experiment then clearly shows that the semi-implicit scheme exhibits the same amount of diffusion irrespective of the time step. In order to properly explain those observations, we have also added a truncation error analysis for the semi-implicit scheme in Appendix A.

Those additions, together with moving the experiment’s description from the caption to the text and clearly splitting the linear advection / two-moment sedimentation experiments into subsections, result in the following

(Section 3.1, line 279):

" *First, we present a linear advection test case, where we simplify to only consider sedimentation of a single quantity ϕ by a prescribed velocity field:*

$$\frac{\partial \phi}{\partial t} = -\frac{\partial}{\partial z}\Big(v\,(z)\,\phi\Big) \quad , \quad v(z) = -\left(\frac{\rho_0}{\rho(z)}\right)^{\gamma} \cdot 15\,\mathrm{m\,s^{-1}} \tag{28}$$

In addition, we use $\rho_0 = 1.225\,\mathrm{kg\,m^{-3}}$, $\gamma = 0.4$, a standard atmosphere for $\rho(z)$, and $\Delta z = 100\,\mathrm{m}$. For $\Delta t = 10\,\mathrm{s}$, this results in the Courant number smoothly increasing from $C = 1.5$ at $z = 0$ to $C = 4$ at $z \approx 19.4\,\mathrm{km}$. Initial conditions are described by a single square wave.

Figure 2 depicts the results from this linear advection test case, showing that the semi-implicit method is significantly more diffusive than the explicit variant. In addition, the numerical solutions with a reduced time step are shown, indicating different behavior of the two methods: In the explicit case, a smaller Δt (while keeping Δz constant) increases numerical diffusion. This can be intuitively understood by Fig. 1, where we show how a cell's content is distributed during a single step; and a smaller Δt simply increases the number of steps until a fixed time is reached. In contrast, the amount of diffusion in the semi-implicit approach remains largely unaffected by Δt. This can be explained by a truncation error analysis (Appendix A), which reveals that the diffusive error scales with $\mathcal{O}\left(\Delta z\, v + \Delta z \Delta t\, v v_z\right)$, where the subscript refers to differentiation. Since v_z is small, cf. Eq. (28), the dominant diffusive error term scales only with Δz and is independent of Δt. Furthermore, since this is a stationary case $v_t = 0$, the entire $\mathcal{O}\left(\Delta t\right)$ error term from Eq. (A22) drops away, leaving only the diffusive error and smaller terms in $\mathcal{O}\left(\Delta z \Delta t + \Delta t^2 + \Delta z^2\right)$ or with small prefactors v_z, v_{zz}. This leads to the almost identical solutions for $\Delta t = 10\,\mathrm{s}$ and $\Delta t = 2.5\,\mathrm{s}$ in the semi-implicit case. "

6) Figure 7 shows differences when using a very small threshold ($10^{-9}\,\mathrm{g/m^{-3}}$), which is almost negligible. What happens when using a more-relevant threshold like $10^{-6}\,\mathrm{g/m^{-3}}$?

(Note: the threshold is actually $10^{-9}\,\mathbf{kg}\,\mathrm{m^{-3}}$, and Fig. 7 is now Fig. 8 in the revised manuscript) First, we want to emphasize that this small threshold ($10^{-9}\,\mathrm{kg\,m^{-3}}$) is not arbitrary, particularly it is used by ICON to determine whether sufficient mass is present to use a nonzero sedimentation speed in the respective level, cf. Eq. (26). To make this clearer, we have added the following sentence (line 457):

"*Only if the mass density exceeds this threshold, a nonzero sedimentation speed is applied.*"

Still, we now additionally provide the same figure but with a 1 000 times larger threshold of $10^{-6}\,\mathrm{kg\,m^{-3}}$ in the Appendix (Fig. C3), which we also refer to in the caption of Fig. 8:

"*The value of q_{crit} is motivated by its use in Eq. (26); a similar analysis using a larger threshold is provided with Fig. C3.*"

7) Figure 4: do you keep a constant dz / dt ratio like in Figure 3? Please clarify it.

Yes, we keep the dz / dt ratio constant; both figures are created from exactly the same experiment. As mentioned before, this experiment (Fig. 3 and Fig. 4) is now contained in its own subsection (3.2), the experiment description is moved from the caption to the text and is slightly adjusted. We believe those changes fully clarify that both figures are created from the same experiment. The figure captions now include that "*Setup details are provided in Sect. 3.2*" (Figs. 3, 4), and the relevant part in Section 3.2 now reads as follows (line 307):

" *... resolution impacts the sedimentation schemes. For investigating that, we compare numerical solutions obtained from a wide range of vertical resolutions, closely resembling a convergence study apart from comparing against the spectral solution that clearly differs from the numerical solutions in the limit $\Delta z, \Delta t \to 0$.*

In more detail, we use the numerical schemes as defined in Sect. 2, except for neglecting all hydrometeor interactions, i.e., $\mathcal{Q}_{\mathrm{CCN}}$ and $\mathcal{Q}^{\Delta t}$ from Eq. (27) are skipped. The initial conditions, consisting of three square peaks and a small nonzero background hydrometeor concentration, are chosen to be exactly representable on the vertical grid of all resolutions. The time step is selected to be sufficiently small to avoid frequent Lipschitz condition violations (to avoid introducing spurious oscillation in the explicit scheme), and is simultaneously refined with Δz, i.e., $\Delta z/\Delta t = 12\,\mathrm{m\,s^{-1}}$ is held constant. Further, $\rho \equiv \rho_0$ is assumed everywhere, and ICON's hail hydrometeor parameters are used as listed in Table 2. Figure 3 depicts hydrometeor profiles from this setup, showing initial conditions, a spectral reference solution, and hydrometeor profiles for three mesh resolutions and numerical configurations. The agreement between numerical and spectral solutions is evaluated using the standard L^1 norm, and drawn as a function of mesh resolution in Fig. 4. "

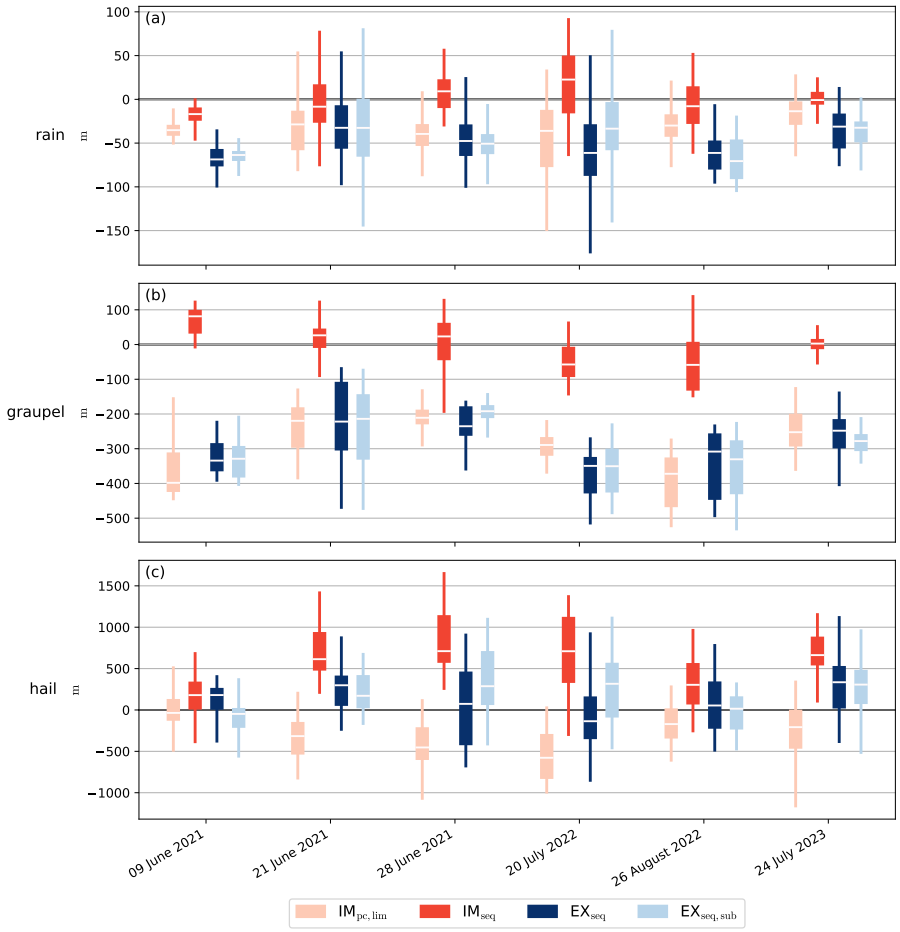

Figure C3: Difference of the mean upper q_{crit} threshold height (i.e., the spatial mean of the highest level's height with $L > 10^{-6}\,\text{kg}\,\text{m}^{-3}$, over the columns where such threshold exists), to the default semi-implicit scheme IM_{pc}; for the time period 14:00–20:00 UTC with 10 min sampling interval. This is similar to Fig. 8, except for using the significantly larger threshold $10^{-6}\,\text{kg}\,\text{m}^{-3}$ instead of $q_{\text{crit}} = 10^{-9}\,\text{kg}\,\text{m}^{-3}$. For rain and graupel, the height difference trends are qualitatively similar to Fig. 8 but roughly half the size. For hail, the explicit configurations approximately match the IM_{pc} variant. In some cases, the less restrictive flux limiter $\text{IM}_{\text{pc,lim}}$ slightly reduces the threshold's height, while the IM_{seq} configuration increases it.

8) In several parts of the paper, it is stated that turbulent diffusion can smooth the profiles of L and N. In ICON NWP there is no turbulent diffusion of hail and graupel.

Thank you for catching that! We were not aware of this fact. It is now clarified where we mentioned turbulent diffusion first (line 213):

" *Furthermore, in non-idealized scenarios, smoothing effects caused by tracer advection and the source terms alleviate the problem by reducing the spatial variations of N and L, thus also of v and the Lipschitz number $\mathcal{B}$. Since turbulent diffusion is not applied to graupel, hail, and rain (only cloud droplets in our configuration), it does not contribute to those smoothing effects where relevant for sedimentation.* "

In addition, we removed the remaining mentions of turbulent diffusion.

9) Page 10, line 240. What do you mean with there is no case distinction?

Equation (25) adjusts N to respect the lower and upper bounds of the mean particle mass, but only if $L > 10^{-12}\,\text{kg}\,\text{m}^{-3}$, otherwise N is set to zero. Where we wrote "*but without the case distinction*", however, it is not first checked for $L > 10^{-12}\,\text{kg}\,\text{m}^{-3}$. We have made that clearer (line 269):

"*Finally, after the microphysical interactions $\mathcal{Q}^{\Delta t}$, the operator $\mathcal{X}$ again enforces mean particle mass limits by*

modifying N, similar to Eq. (25) but without the case distinction, so that N is always set to $\text{clamp}\left(N,\ \frac{L}{\overline{\overline{x}}_{\max}},\ \frac{L}{\overline{\overline{x}}_{\min}}\right)$ *regardless of the value of L.*"

10) This is just a suggestion. If you want to show that comparable results in NWP are obtained with both schemes you could show the one-hour precipitation map, one hour after the simulation start for one case study. This could enhance the confidence in the explicit scheme and show that the differences in roughness are not relevant for typical NWP applications.

That is an interesting idea, however we think a simulation restart with changed microphysics at some time during the afternoon would be required instead, since there is only limited precipitation in the first hours after the simulation start at midnight (in addition to still being in the spin-up phase).

Furthermore, the second referee (Ulrich Blahak) has suggested an addition to our paper with a comparable goal. We have implemented his suggestion instead, and just refer to his comment (number 24) below.

11) Why do you write the approximate symbol in Equation (6)?

We believe it was used to emphasize that the power law itself is already an approximation / parameterization of actual terminal fall speeds. We have now changed it to the equal symbol; however we would be fine with either option.

12) I think there is a mistake in Equation (12). It should be $0.5(v_k^n + v_{k-1}^{n+1})$.

No, this is not a mistake: $\widetilde{v}_k^{(n+1)} := \frac{1}{2}(v_k^{(n)} + v_{k-1}^{(n)})$ is actually the approximation currently used in ICON. Notably, it differs from this scheme's original implementation in the COSMO one-moment scheme (Doms et al., 2021, Eq. (5.18)), which is similar to your proposed change, except for first averaging and then evaluating v: $\widetilde{v}_k^{(n+1)} = v\left(\frac{1}{2}(\phi_k^{(n)} + \phi_{k-1}^{(n+1)})\right)$. However, we agree that this approximation deserves a bit more attention: We actually ran into some issues in the single-column experiments where exactly the difference between taking the velocity $v_{k-1}^{(n)}$ or $v_{k-1}^{(n+1)}$ is relevant. This is already explained at line 253 (unchanged except for removing the mention of turbulent diffusion):

"*In idealized single-column experiments and high Courant numbers in combination with the semi-implicit scheme, such a threshold q_{crit} may actually prove problematic for the velocity approximation in Eq. (12). At the leading edge of a precipitation column, where L drops below q_{crit}, this threshold can only propagate by two levels per time step, which results in a strong shock wave if the actual propagation speed is larger. This could be remedied by either skipping the q_{crit}-based case distinction in Eq. (25), or using a different approximation for $\widetilde{v}^{(n+1)}$, e.g., $\widetilde{v}_k^{(n+1)} = 0.5 \cdot \left(v_k^{(n)} + v_{k-1}^{(n+1)}\right)$, which incurs slightly higher computational cost from additionally computing the velocities $v^{(n+1)}$. However, in practice this issue occurs extremely rarely, as it is almost impossible to uphold those problematic conditions for any significant amount of time, particularly as the three-dimensional microphysical tracer fields are also mixed and smoothed through tracer advection and the turbulent diffusion scheme in-between each microphysics step.*"

We think it might make sense to already reference this where we define the velocity approximation used in ICON, so we have added the following after Eq. (12) (line 144):

"*We should add that the velocity approximation in Eq. (12) is clearly different from the original COSMO implementation, where $\widetilde{v}_k^{(n+1)} = v\left(\frac{1}{2}(\phi_k^{(n)} + \phi_{k-1}^{(n+1)})\right)$ was used (Doms et al., 2021, p. 52); especially note how the ICON implementation only takes values from time step n. In Sect. 2.4, we will mention how an interaction of this approximation with Eq. (26) could cause an artificial shock wave, although this is almost irrelevant in practice.*"

13) Why do you write the super index **lim** and **lim2** in the right-hand side of Equations (13) and (14)?

We are unsure whether this question is about the distinction between **lim1** and **lim2** that merely denote two variants of the flux limiter that is referred to as a generic **lim** in all other equations, or about why the limited fluxes also appear on the right-hand side.

For the former, we added a sentence that should make the distinction clear (line 158): "*Note that we use the generic* $^{\text{lim}}$ *superscript to refer to either of the two flux limiters from Eqs. (13) and (14).*"

For the latter: The value on the left-hand side, $(v\phi)_k^{(n),\text{lim}}$, defines the limited flux for level k, whereas on the

right-hand side we merely use the limited flux from *the level above*, $(v\phi)_{k-1}^{(n),\mathrm{lim}}$. This is unproblematic, since the semi-implicit scheme updates the values level-wise starting from the top of the domain, and on the highest level the in-flowing flux is just set to zero from the BCs. Further, those flux limiters just arise from solving $\phi_k^* \geq 0$ for the flux $(v\phi)_k^{(n),\mathrm{lim}}$, as given in Eq. (10). Somehow replacing $(v\phi)_{k-1}^{(n),\mathrm{lim}}$ with $(v\phi)_{k-1}^{(n)}$ on the right-hand sides of Eqs. (13) or (14) would then be unable to guarantee $\phi_k^* \geq 0$. Put another way, the limited flux $(v\phi)_{k-1}^{(n),\mathrm{lim}}$ on the right-hand sides of Eqs. (13) and (14) comes from Eq. (10). And if we were to use $(v\phi)_{k-1}^{(n)}$ instead of $(v\phi)_{k-1}^{(n),\mathrm{lim}}$ in Eq. (10), conservation of mass would be destroyed.

Response to Ulrich Blahak (referee #2)

Comments to the Authors

This paper analyses and compares two numerical hydrometeor sedimentation schemes which are offered as options in the ICON model's two-moment bulk cloud microphysical scheme. As the original author of the herein examined explicit scheme, first I would like to thank the authors for this overall good and useful paper. I especially like the graphical explanation of the explicit FFSL method. The experiments are well designed and the conclusions are well founded. In detail, I see some room for improvement, which I would consider as minor revisions: for example, the nature of the analytic (?) / numerical (?) reference solution for the idealized sedimentation experiments need more explanation, and the paper and its conclusions would profit from adding more informations on the overall effect on practically relevant model outputs like 1-h rain accumulation, 1-h hail accumulation and radar reflectivity at relevant heights above 500 m AGL.

Before my detailed comments, I would like to give some historical information which might be useful background and might even be mentioned somehow in the introduction. As stated in my 2020 documentation of the explicit schemes, the explicit "boxtracking" scheme was meant as a first improvement over the traditional explicit scheme, which was at that time the only sedimentation option for the two-moment scheme and which showed worse "spiky" and "rough" behaviour at Courant numbers > 1, especially close to the ground, where the model layers are very thin. It's main flaw was the approximation of the fallspeed $v_{k-l} == v_{k+1/2}$. The explicit boxtracking scheme has been developed in the COSMO-model framework and takes into account the "true" fallspeed of each box $k - l$ (therefore I called it "boxtracking"). The implicit solver existed only for the one-moment scheme, in both the COSMO and ICON implementation of the two-moment microphysics. Lateron, Axel Seifert implemented the implicit scheme also for the two-moment microphysics in the ICON framework, and this became our standard scheme during ICON-RUC development. We already noticed the high diffusivity, but as we did not find a significant impact on practically relevant fields in real-case weather forecasting, we favored the implicit scheme due to its conceptual advantages concerning the hydrometeor interactions at large Courant numbers, which are also mentioned in the present paper.

We thank Ulrich Blahak for this useful background and the positive and constructive comments, and we will address the detailed comments below.

The concerns regarding the reference solution are already addressed in our answer to the first detailed comment of anonymous referee #1, and we have introduced a new section (4.1) that shows and discusses a few practically relevant model outputs (addressed in the detailed comment number 24 below). In the introduction, we have added the following sentence to provide a bit more background (line 59):

" *The explicit scheme considered here is documented and referred to as the "boxtracking" scheme by Blahak (2020), which was meant as a first improvement over a scheme with significantly flawed fall speed approximation in the flux calculation.* "

Detailed comments

1) Abstract: "... we caution that in the future, finer grid resolution may result in insufficient diffusion, ..."

I think this statement cannot be made in general, as it depends on adaptions of vertical layers and model time step which are done simultaneously alongside a reduction of horizontal grid spacing. For example, if just the horizontal grid spacing and the time step are reduced, but the vertical levels are not touched (which is sometimes the case), then I would expect more diffusion from the sedimentation scheme. Similar statements are also made elsewhere in the manuscript. You could relax the statement in a way that you discuss that a change of diffusion depends on changes to the vertical resolution and the model time step and may change in

the one or other direction, when model resolution is enhanced in the future.

Thank you for catching that! We refer to our response to the fourth detailed comment of anonymous referee #1, who has raised the same issue.

2) Line 48: "... shown by runtime measurements in Table 1." Add a remark that this behaviour will be explained/examined in more detail in later section 2.2

Indeed, that would be helpful. We have modified the sentence (line 47): "*However, this explicit variant performs much better on GPUs, shown by runtime measurements in Table 1, which will be discussed in detail in Sect. 2.2.*"

3) Line 91: "... to account for the increasing air density rho ..." –> better: " ... to account for the dependence of the terminal fall speed on air density rho ..."

Thank you, this is changed as suggested (line 94).

4) Line 108: "... deliberate use of diffusive numerical schemes ..." While I completely agree with the statement, to me it is unclear what an "optimal" amount of diffusion might be, if at all, as this depends on many things. So how do we decide what amount of diffusion is appropriate? Maybe you could add some brief discussion of your view on this point and the associated uncertainty, because the paper compares schemes with different amount of diffusion.

After our description of the two-moment scheme, we have added the following paragraph (line 113):

" *Of course, then the question of what the optimal amount of diffusion is arises. When only relying on numerical diffusion, the specific amount typically depends on the advection speed and discretization (Δz and/or Δt), and thus can vary significantly across the domain. Generally, too little diffusion will result in spurious shock waves, whereas too much diffusion produces overly smooth fields that may be unable to capture fine structures of clouds, and reduces size sorting. It should be noted that the latter may actually be desired, since size sorting is often too pronounced in two-moment schemes (Milbrandt and Yau, 2005; Mansell, 2010). To find the right balance between those effects, in theory, we would suggest deriving the optimal diffusion coefficient directly from the spectral formulation, e.g., by computing a Taylor expansion in space of the spectral solution's moments, giving rise to an ideal local diffusion coefficient that depends on the moment m and hydrometeor concentrations N, L themselves. In principle, such a coefficient could be combined with knowledge about the diffusive error terms of the numerical schemes used in sedimentation and tracer advection, allowing a tight control over diffusion across resolutions. However, the benefits of such a complex approach appear questionable, especially compared to all other approximations and uncertainties that exist in the parameterizations of cloud microphysical processes.* "

5) Line 110: please explain also Q as shortcut for Q_N and Q_L.

Thank you, we missed that. We have added the source term to this sentence and slightly reformulated it for improved readability (line 126): "*For clarity and conciseness, we will use ϕ to describe both N and L for all hydrometeor classes. Likewise, we will use the generic source term Q and velocity v; these refer to the source term and velocity function, respectively, for the respective moment and hydrometeor class.*"

6) Line 120: "$v_k^{(n+1)}$" –> "$\tilde{v}_k^{(n+1)}$"?

We are not sure what the issue is. We cannot find any missing tilde, and think the sentence explaining that "*the implicit velocity $v_k^{(n+1)}$ was replaced by the explicit approximation $\widetilde{v}_k^{(n+1)}$*" (line 139, Eq. (12)) is clear.

7) Line 147: "This accounts for nearly all the runtime difference ..." To support this statement, please add the timing numbers for the semi-implicit sequential scheme in comparison to the full semi-implicit and explicit scheme in a suitable way.

We now introduced a third column in Table 1 that lists timings for the semi-implicit sequential scheme. Since we observed slightly, but systematically higher runtimes now, compared to when we initially performed the timing measurements for the first two columns, we have repeated those experiments and replaced the times to ensure consistency.

We also reworded the sentence in question to be more precise, and added that the runtime differences are not

inherent to the scheme but rather a limitation of the current implementation (line 169):

"*On GPUs, this accounts for over 85 % of the runtime difference between (...). Still, we see no fundamental reason why all variants of the semi-implicit scheme could not reach GPU runtimes similar to the explicit scheme. This would, however, require a rather substantial rewrite of the implementation.*"

8) Figure 1: Some sub- and superscripts are missing, at least in my pdf version: "$z-z$" should be "$z_{up}-z_{low}$", "$v_2^{()}$" should be "$v_2^{(n)}$"

Indeed, we can see the same in the pdf file of the preprint: Although the characters exist, they appear invisible. In our submitted manuscript, however, everything looks fine. If there is actually an issue with this figure, we are happy to engage with the editors. For completeness, we also include a copy of this figure in png format here with Fig. R1.

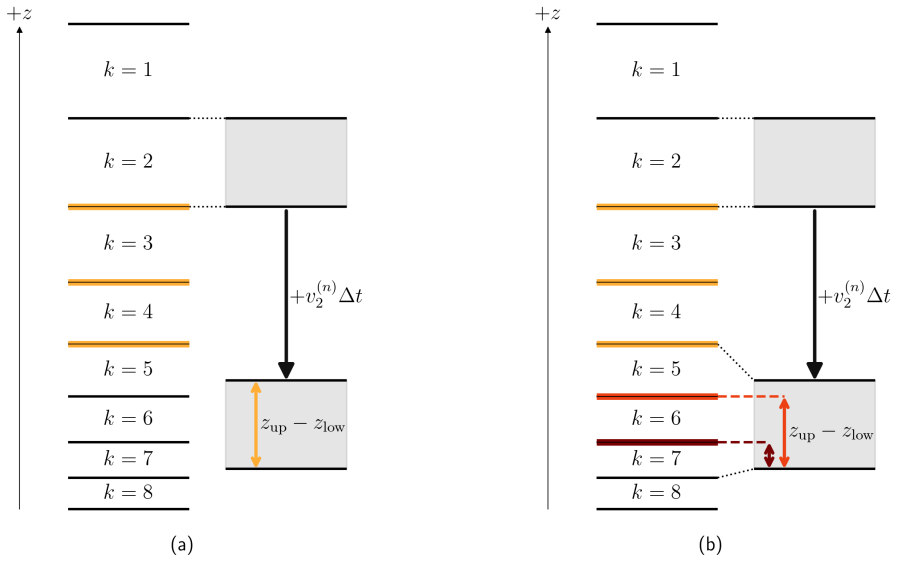

Figure R1: This is the png version of Fig. 1.

9) Line 193 ff: Please add in a suitable way the information that the substepping is optionally implemented by an internal code switch, which is disabled by default because of reproducibility problems in current ICON. You should clearly state in the following paragraph that you found the reason for the reproducibility bug (missing global mpi max reduction of N_sub), fixed it in your code version and reported it to the ICON developers (I'm one of them, so I know now :-) Thank you for finding it!).

Thank you! We have inserted the following sentence (line 219):

" *This is controlled by an internal code switch, which is disabled by default because of reproducibility problems in the current ICON version when the domain decomposition changes, i.e., when the number of processes is modified.* "

We have then slightly edited the following paragraph (line 226):

" *... Further, the aforementioned reproducibility problem is caused by the computation of* $\min_k(\Delta z_k)$*, which is done over the local domain (determined by partitioning the entire simulation region according to the number of processes). Therefore,* $\min_k(\Delta z_k)$ *might vary slightly across the processes, depending on the domain decomposition. This issue is reported to the ICON developers; and to improve the reproducibility of our simulations, we manually fix* N_{sub} *to the highest value encountered across the entire simulation domain.* "

10) Line 2019: Please define the "clamp()" operator, because not everyone from the meteorological community will be familiar with it.

We have now defined "clamp" in Eq. (24) (line 247)

$$\text{clamp}\left(y,\ y_{\min},\ y_{\max}\right) := \min\left(\max\left(y,\ y_{\min}\right),\ y_{\max}\right) \tag{24}$$

just before its first use in Eq. (25).

11) Line 247: Please explain the "spectral solution" in more detail. Was it obtained by a bin scheme or by an analytic solution of Eq. (1)?

Thank you. We refer to our response to the first detailed comment of anonymous referee #1, who has raised the same issue.

12) Line 249: Please mention the initial condition with it's single block of hydrometeors. This is different to your next test with 3 initial blocks (Figure 3).

Thank you, this should be much clearer now, after separating the two experiments into Sections 3.1 and 3.2. In Section 3.1, we have added (line 284) "*Initial conditions are described by a single square wave.*"

13) Line 252: "... future resolution increases in accordance ..." –> "... future resolution increases (also in the vertical) in accordance ..."

Thank you, we have added "*(also in the vertical)*" as suggested (line 306).

14) Line 254: "... showing initial conditions, ..." –> "... showing initial conditions with 3 peaks, ..."

In the new Section 3.2, we now describe the initial conditions in more detail (line 312):

" *The initial conditions, consisting of three square peaks and a small nonzero background hydrometeor concentration, are chosen to be exactly representable on the vertical grid of all resolutions.* "

15) Line 254: Is the spectral solution the same method as for figure 2? Please explain.

By splitting up the linear advection and two-moment scheme experiments into separate subsections (3.1, 3.2) and better describing the two experiments in the text, we believe it is now obvious that in Fig. 2, we simply show the analytical solution of the solved linear advection equation.

Since we now include a description of our spectral solution in Section 3.2 (line 298), it should be equally clear that this spectral solution is used for Figs. 3 and 4.

16) Captions of Fig. 3 and Fig. A1: "... graupelhail_cosmo5 in the file src/atm_phy_schemes/..." Please do not reference the code, but put the relevant parameter values into a table.

We have introduced a new table that lists all hail and graupel parameters that are relevant for sedimentation (Table 2). The captions of Fig. B1 now reads "*... as listed in Table 2*"; and for Fig. 3, the same is now included in the text (line 314).

17) Caption to Fig. 4: "... for spatial resolutions ranging from Δz = 5m ... in 2x increments" –> "... for spatial resolutions Δz = 5, 10, 20, 40, ..., 1280m. "

Thank you, we changed the caption of Fig. 4 as suggested.

18) Caption to Fig. 4: "... and further details are provided by Fig. 3." –> "... and further details have already been provided in Fig. 3"

Since we moved the experiment's description to the text, the captions of both Figs. 3, 4 now refer to the text:"*Setup details are provided in Sect 3.2.*" We still write "are provided" instead of "have already been provided" since the ordering of text and figures is less clear; but of course the editor is free to adjust this as necessary.

19) Line 275: "... show, ..." –> "... show up, ..."

Thank you, we changed this as suggested (line 340).

20) Line 279: Which individual summer days? Please list the dates for reproducability of your work.

The dates are already visible in Figs. 6, 8, and C2; and we think listing them all in the text is not particularly helpful and a bit disrupting. Still, to make that more clear, we now explicitly refer to such a figure at our first mention of the six days (line 344): "*... six individual summer days (listed in Fig. 6) with ...*"

21) Section 4.1: The motivation and illustration for investigating the roughness would benefit from an exemplary figure. You could add a zoom-in to a precip rate field from one of your experiments to illustrate it by spatial noise, because noise in time (=roughness) translates into noise in space under horizontal transport.

Thank you, it would definitely help to better motivate the roughness. In Fig. 5, which we added in response to comment 24 (see below), we have included a few time series of precipitation rates at grid points. While this is not exactly your suggestion, we believe it addresses the concern well; especially since we now discuss this figure in the beginning of Sect. 4 and use it as motivation to analyze the precipitation rate extrema and roughness.

22) Line 386: The amount of numerical diffusion depends also on the time step (= how often the scheme is called)

Yes, definitely; we forgot to mention that there. Thank you! We have added it to this sentence (line 475):

"*Since the numerical diffusion is not parameterized, its amount heavily depends on the time step, vertical resolution and specific scheme in question; (...)*"

23) Line 409: "This inevitably results in reduced numerical diffusion" (See above point 1)

We have modified this sentence and summarized our findings as addressed in previous comments (line 499):

" *(...) If only the horizontal resolution is increased, the ensuing time step reduction will lead to more numerical diffusion in the explicit scheme, but leave the semi-implicit scheme largely unaffected. This is noteworthy, as it increases the similarity between the two sedimentation methods, thus rendering the explicit scheme more viable. Conversely, also increasing the vertical resolution results in reduced numerical diffusion for both schemes, which may become problematic for the explicit scheme due to the loss of smoothing capacity for (...) In all cases, the smaller time step leads to reduced splitting errors in the source terms, which could necessitate small adjustments of tuned parameters.* "

24) Conclusions:

I agree fully to your statement in line 406ff that "... in full model simulations those issues seem to be mitigated by ..." and "... we find that the explicit scheme can be safely used on GPUs ...".

Since this is one of your main messages for the community, please add a new section right before the conclusions section, where you qualitatively show/compare real-case results for practically relevant forecast fields like 1-h precipitation accumulation, 1-h hail accumulation, and radar reflectivity at relevant heights $>$ 500 m AGL, e.g., dbz_850 (because model verification and radar data assimilation is usually based on observations from those and larger heights). This should be not too complicated and time-consuming, because I would think that you already have these fields on disk from your real-case experiments. You could plot zoom-ins to these fields of one example time step of one of your real-case experiments, and compare the fully semi-implicit, the sequential semi-implicit and the explicit scheme. My expectation would be that the three methods show some differences, but that these differences are negligible compared to other meteorological forecast uncertainties, and this would be a clear illustration of your point.

Thank you for this suggestion! We have decided to insert such a figure (Fig. 5) in the beginning of Sect. 4, and also use it as motivation to look at the precipitation rate extrema and roughness in the following. Specifically, we show the accumulated precipitation over the same 6 h period used in all other figures, and then provide a zoom-in view of a single storm where we show the 1 h accumulated hail, radar reflectivity at 2 km height (since the highest peak in this area is at approximately 1.5 km), and the instantaneous precipitation rate at a time point. In addition, a few precipitation rate time series are also shown for a few selected grid points, as response comment 21 above.

Since Fig. 5 only shows three out of the five configurations, the other two are also provided with Fig. C1 in the Appendix.

The following text is the entirely new Section 4.1 that discusses this new figure (line 357):

" *We start by providing a map view of the 20 July 2022 case in Fig. 5, where we compare precipitation and radar reflectivity of the IM_{pc}, IM_{seq}, and EX_{seq} configurations (the $IM_{pc,lim}$ and $EX_{seq,sub}$ configurations are provided in Fig. C1). On this day, several thunderstorms with large hail were observed over the Jura mountains at the*

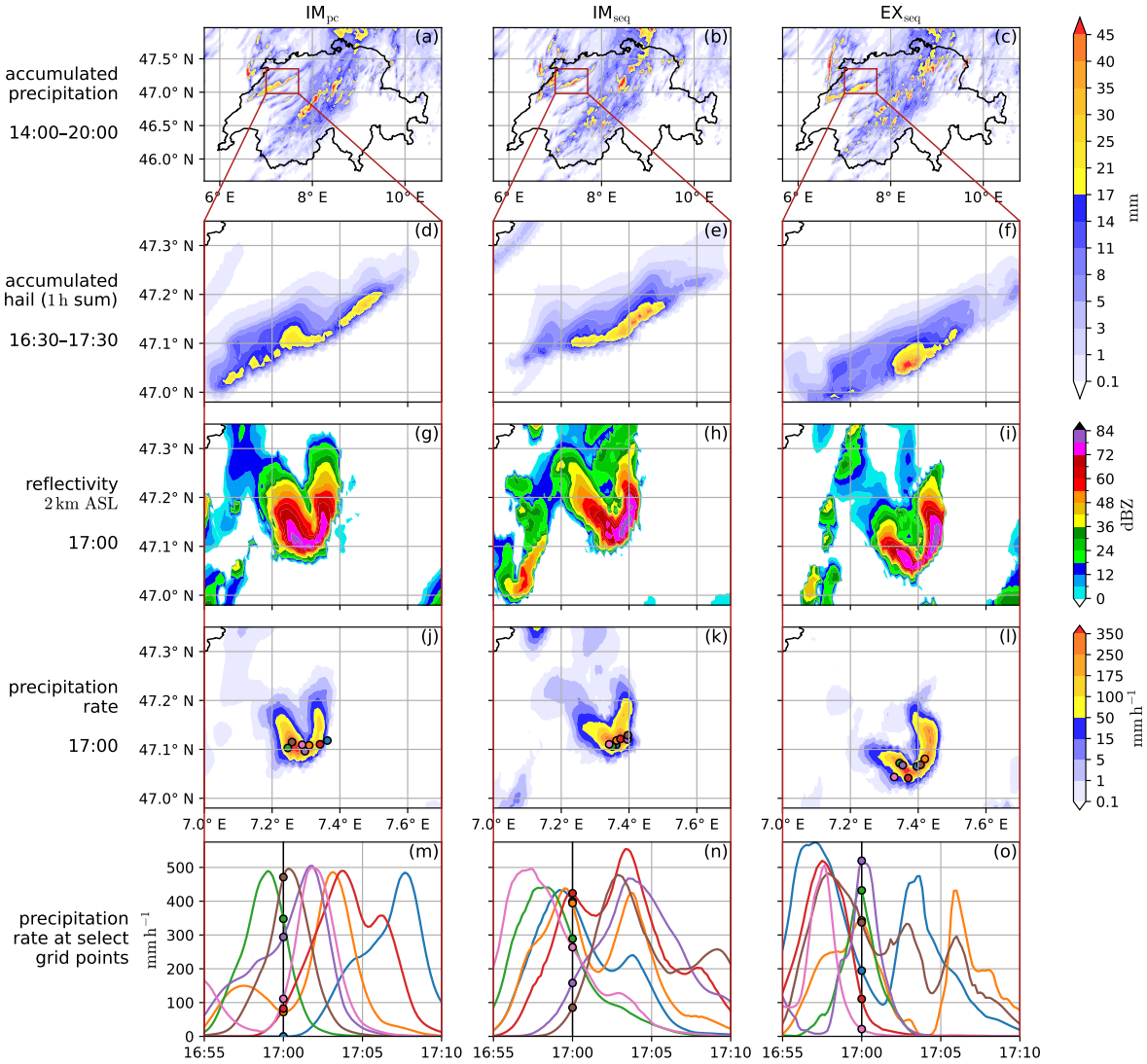

Figure 5: For the 20 July 2022 case and the $\mathrm{IM_{pc}}$, $\mathrm{IM_{seq}}$, and $\mathrm{EX_{seq}}$ configurations, the accumulated precipitation from 14:00–20:00 UTC over the entire simulation domain is shown in the first row (a)–(c). The following rows give a zoom–in view of a severe storm over the Jura mountains, specifically the 1 h accumulated hail (d)–(f), radar reflectivity at 2 km ASL (g)–(i), and instantaneous precipitation rate at 17:00 UTC (j)–(l). The last row (m)–(o) displays the time evolution of precipitation rates for a few select grid points whose locations are marked in the row (j)–(l) above. The configurations $\mathrm{IM_{pc,lim}}$ and $\mathrm{EX_{seq,sub}}$ are shown in Fig. C1.

France–Switzerland border, around Basel, and the Prealps from Bern to Zug[1]*. Although slightly different in detail, all configurations predict storms over the Jura mountains (in the northwest in Fig. 5a–c), and in a diagonal band from the southwest to the northeast of Switzerland. In a zoom-in view of a single storm, the* 1 h *accumulated hail is shown in Fig. 5d–f. Both configurations with sequential source term treatment (IM_{seq}, EX_{seq}) result in higher maxima of accumulated hail compared to the predictor-corrector variant IM_{pc}. This is not a truncation effect of the time window, as most precipiation occurs in the window's center at around 17:00. In addition, the storm's track is slightly shifted south in the EX_{seq} case. Next, we show the radar reflectivity at* 2 km *height at time 17:00 in Fig. 5g-i, and the corresponding instantaneous precipitation rate in Fig. 5j-l. Notably, all three configurations exhibit a similar U–shaped structure. Finally, for a few select grid points, we show how the precipitation rate evolves during a* 15 min *window in Fig. 5m-o. All configurations exhibit precipitation rates in excess of* 300 mm h^{-1}*, however only for a few minutes as the storm moves and eventually dissipates; e.g., on average* 300 mm h^{-1} *for* 5 min *results in* 25 mm *of precipitation on the ground. However, particularly for the EX_{seq} configuration, the precipitation rate appears less*

[1] `https://www.sturmarchiv.ch/index.php?title=Extremereignisse_2022#Juli`, accessed 06 Nov 2025

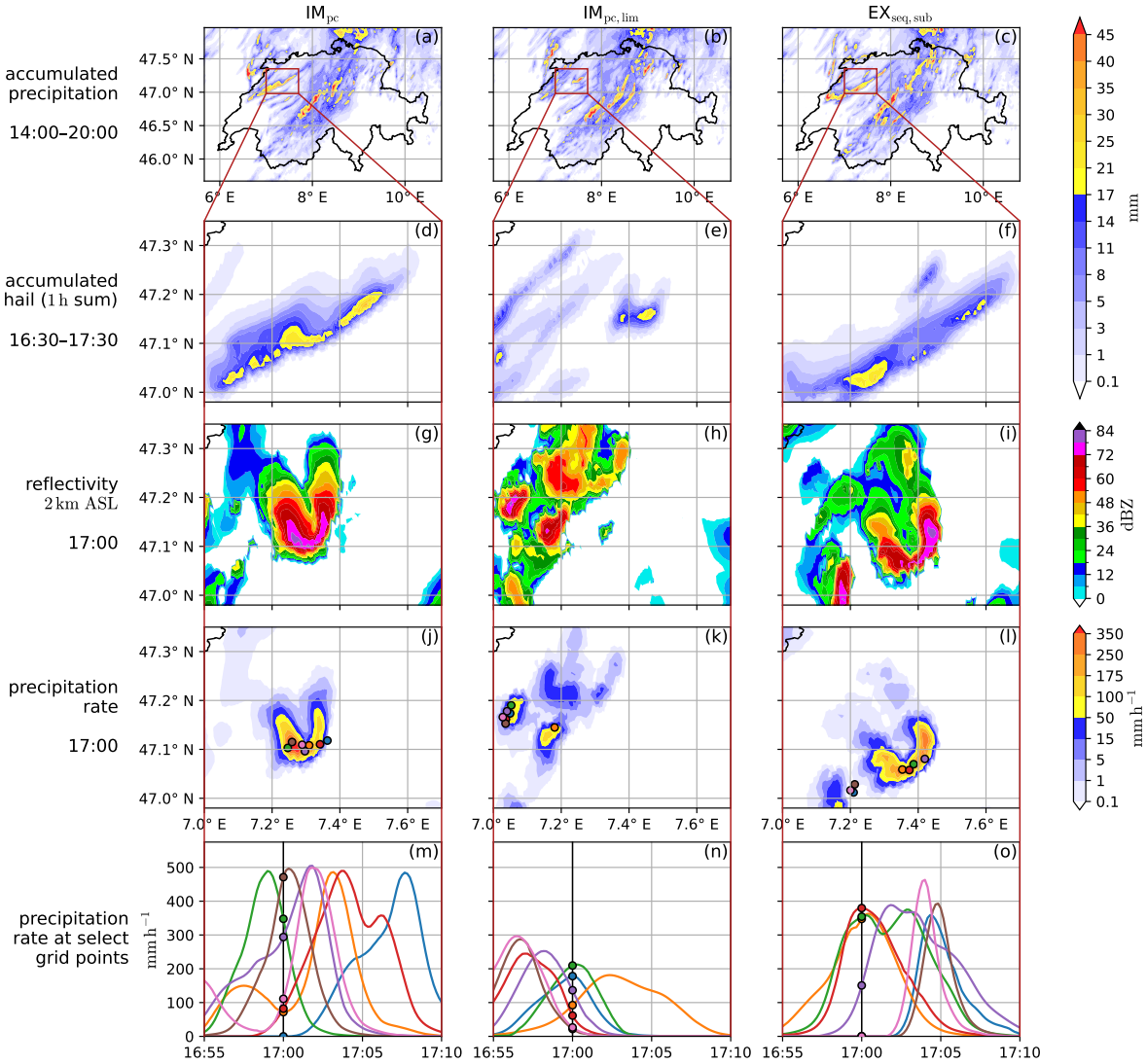

Figure C1: For the 20 July 2022 case and the $\mathrm{IM_{pc}}$, $\mathrm{IM_{pc,lim}}$, and $\mathrm{EX_{seq,sub}}$ configurations, the accumulated precipitation from 14:00–20:00 UTC over the entire simulation domain is shown in the first row (a)–(c). The following rows give a zoom–in view of a severe storm over the Jura mountains, specifically the 1 h accumulated hail (d)–(f), radar reflectivity at 2 km ASL (g)–(i), and instantaneous precipitation rate at 17:00 UTC (j)–(l). The last row (m)–(o) displays the time evolution of precipitation rates for a few select grid points whose locations are marked in the row (j)–(l) above.

smooth, i.e., includes small oscillations at various points, with steeper gradients and more rapid changes compared to the default implicit variant IM_{pc}.

Notably, out of the five configurations listed in Table 4, the storm cell shown in Fig. 5d–o deviates significantly only in the configuration with the improved flux limiter $IM_{pc,lim}$ (Fig. C1), where it produces less intense precipitation and hail, and lacks the U–shaped structure. We suspect this discrepancy is largely coincidental, since inspecting other storm cells reveals that different configurations occasionally exhibit similar outliers. As the flux limiter improvement is only a minor numerical adjustment, this deviation may rather originate from the inherent sensitivity of such individual convective cells after 17 h of lead time. Especially in the context of this broader meteorological forecast uncertainty, the other configurations produce remarkably similar outcomes. Still, we clearly see differences in the roughness of precipitation rates, and the accumulated hail may hint at slight shifts in the precipitation (rate) distribution, and/or the ratio between hydrometeor classes.“

Response to Astrid Kerkweg (CEC1)

Dear authors,

to meet all requirements w.r.t. code provision, you need to provide also the code modification in an open way in a longterm archive. The ETHZ gitlab is neither open nor does it fulfill the requirements for a longterm archive.

Best regards,

Astrid Kerkweg (GMD executive editor)

Thank you for bringing that to our attention. We have now archived our code modifications as separate git patch files with Zenodo, properly cited them in the "Code and data availability" part. We quote the updated "Code and data availability" section (line 514):

" *We used the open-source ICON model code version 2024.10 for our simulations, available at* `https://doi.org/10.35089/WDCC/IconRelease2024.10` *(ICON partnership (MPI-M, DWD, DKRZ, KIT, and C2SM), 2024) or* `https://icon-model.org`*. The code modifications to obtain all model configurations are provided in Bolt and Omanovic (2025b) (*`https://doi.org/10.5281/zenodo.17728556`*). Model data are available from Bolt and Omanovic (2025a) (*`https://doi.org/10.5281/zenodo.17782126`*), and plotting scripts, including all code for reproducing the single-column sedimentation experiments, can be obtained from Bolt and Omanovic (2025c) (*`https://doi.org/10.5281/zenodo.17782140`*).* "

References

Doms, G., J. Förstner, E. Heise, H.-J. Herzog, D. Mironov, M. Raschendorfer, T. Reinhardt, B. Ritter, R. Schrodin, J.-P. Schulz, and G. Vogel (2021). *COSMO-Model Version 6.00: A Description of the Nonhydrostatic Regional COSMO-Model - Part II: Physical Parametrizations*. DOI: 10.5676/DWD_PUB/NWV/COSMO-DOC_6.00_II. URL: https://www.dwd.de/EN/ourservices/cosmo_documentation/pdf_docu_v6_0/2_cosmo_physics_6_00_en.pdf.